Advances in Technological Design to Optimize Exposure and Improve Image Quality

Gutierrez Rios, Daniel Fernando; Zaidi, Habib

How to cite

GUTIERREZ RIOS, Daniel Fernando, ZAIDI, Habib. Advances in Technological Design to Optimize Exposure and Improve Image Quality. In: Radiological Safety and Quality: Paradigms in Leadership and Innovation. Lau, Lawrence. & Ng, Kwan-Hoong (Ed.). Dordrecht : Springer, 2013. p. 177–202. doi: 10.1007/978-94-007-7256-4_10

This publication URL: https://archive-ouverte.unige.ch/unige:33220
Publication DOI: 10.1007/978-94-007-7256-4_10

Chapter 10
Advances in Technological Design to Optimize Exposure and Improve Image Quality

Daniel F. Gutierrez and Habib Zaidi

Abstract Multimodality imaging is playing a key role in the clinical management of patients in routine diagnosis, staging, restaging and assessment of response to treatment, surgery and radiation therapy planning of malignant diseases. The complementarity between anatomical (CT and MRI) and functional/molecular (SPECT and PET) imaging modalities is now well recognized and the role of fusion imaging is widely used as a central piece of the general tree of clinical decision making. Moreover, dual-modality imaging technologies including SPECT/CT, PET/CT and nowadays PET/MR represent the leading component of a modern healthcare facility. There have been significant advances in data acquisition along with innovative approaches to image reconstruction and processing with the aim to improve image quality and diagnostic information. However, CT procedures involve relatively high doses to the patient, which triggered many initiatives to reduce the delivered dose particularly in paediatric practice.

This chapter discusses the state-of-the-art developments and challenges of multimodality medical imaging technologies and dose reduction strategies. Future opportunities and the challenges limiting their adoption in clinical and research settings will also be addressed.

D.F. Gutierrez
Division of Nuclear Medicine and Molecular Imaging, Geneva University Hospital, Geneva CH-1211, Switzerland

H. Zaidi (✉)
Division of Nuclear Medicine and Molecular Imaging, Geneva University Hospital, Geneva CH-1211, Switzerland

Geneva Neuroscience Center, Geneva University, Geneva CH-1211, Switzerland

Department of Nuclear Medicine and Molecular Imaging, University of Groningen, University Medical Center Groningen, 9700 RB Groningen, Netherlands
e-mail: habib.zaidi@hcuge.ch

L. Lau and K.-H. Ng (eds.), *Radiological Safety and Quality: Paradigms in Leadership and Innovation*, DOI 10.1007/978-94-007-7256-4_10,

Keywords Hybrid imaging • Image quality • Multimodality imaging • Patient dose • Radiation exposure

1 Introduction

The fields of diagnostic radiology and medical imaging cover a plethora of techniques that are vital for evaluating and managing patients who require medical care. Conventional imaging techniques such as plain film radiography and more recent techniques such as x-ray computed tomography (CT) and magnetic resonance imaging (MRI) are used to evaluate a patient's anatomy with sub-millimeter spatial resolution to discern structural abnormalities and to evaluate the location and extent of disease. These methods offer relatively fast scan times, precise statistical characteristics, and good tissue contrast especially when contrast media are administered to the patient. In addition, x-ray fluoroscopy and angiography are used to evaluate the patency of blood vessels [7], the mechanical performance of the cardiovascular system, and structural abnormalities in the gastrointestinal or genitourinary systems. Similarly, CT and MRI can be performed with cardiac gating to the heart at different phases of the cardiac cycle. Computed tomography recently has experienced a significant increase in utilization with the advent of multislice helical scanning techniques that cover a large region of the patient's anatomy with a single breath-hold and with scan speeds that can capture both the arterial and venous phases of the contrast bolus. These increased scan speeds enhance patient comfort, and contribute to patient throughput and cost effectiveness [31].

In contrast to the anatomical imaging techniques described above, functional imaging methods including planar scintigraphy, single-photon emission computed tomography (SPECT), positron emission tomography (PET), and magnetic resonance spectroscopy (MRS), assess the regional differences in the biochemical status of tissues. In nuclear medicine, including SPECT and PET, this is done by administering the patient with a biologically active molecule or pharmaceutical, which is radiolabelled and accumulated in response to its biochemical attributes. Nuclear imaging relies on the tracer principle in which a minute amount of a radiopharmaceutical is administered to assess physiological function or the biomolecular status of a tissue, tumour, or organ within the patient. The volume of the radiopharmaceutical used is sufficiently small such that its administration does not perturb normal organ function. However, the radiopharmaceutical produces a radioactive signal that can be measured, and ideally imaged, by using an external array of radiation detectors. By design, the radiopharmaceutical has a targeted action, allowing it to be imaged to evaluate the specific physiological processes in the body. There are now many radiotracers which are suitable for clinical diagnosis, with additional radiotracers available for in vivo as well as in vitro biological experimentation. Extended descriptions of these techniques are well documented [14, 17, 78, 82].

2 Overview of Medical Imaging Techniques

2.1 Projection Imaging (2D) Techniques

Projection imaging was the first non-invasive imaging technique developed by Wilhelm C. Röentgen following the discovery of x-rays in 1895. It was quickly applied as a clinical tool, not only to demonstrate fractures or other anomalies of hands and arms, but also for surgical purposes. This is a transmission procedure involving the acquisition of a two-dimensional image of a body region. The x-rays produced by the x-ray tube on one side of the patient pass through the body. The image formation is based on the differential penetration of the x-rays, with the contrast of the image being the consequence of the different paths of the radiation going through different tissues. For example, bones cause significantly higher attenuation than soft tissues, resulting in a smaller exposure of the regions where x-rays encounter bone and thus the resulting image is whiter than soft tissue.

Mammography is a procedure specially designed to detect abnormalities in the breast, which can be very difficult owing to two reasons: lesions can be small and the density difference between them and breast tissues is also very small.

Fluoroscopy is a technique where x-ray images are acquired in a dynamic or real-time mode. The name of this technique comes from the fluorescence that Thomas Edison saw while looking at glowing plate screens of calcium tungstate bombarded with x-rays. The first detectors used on these systems were made of image intensifiers coupled to television screens, while the actual systems are composed of flat panel detectors based on thin film transistors (TFT) that are replacing image intensifiers.

2.2 Tomographic Imaging (3D) Techniques

The drawback of conventional radiography is that it does not provide any depth information when 3D objects are projected onto 2D detector geometries. Tomographic imaging presents the advantage of circumventing this limitation through 3D image reconstruction of the region examined to provide series of 2D image slices of the body. For this reason, it was predicted that tomographic imaging techniques will likely replace planar imaging in the future [2]. This remains a controversial topic, which is still being debated [7, 50].

The first tomographic imaging system was introduced by David Kuhl and Roy Edwards in 1965 [11] representing the departure of tomographic imaging in nuclear medicine (SPECT) as well as transmission imaging with radionuclides (^{131}I and ^{241}Am). Later, Sir Godfrey Hounsfield introduced the concept of computed tomography (CT) based on transmission of tube generated x-ray beam [34].

Computed Tomography (CT)

Although the first CT device was introduced by Hounsfield in 1973 [34], the mathematical principles of the filtered backprojection are much older and stem from radioastronomy-related research by Johan Radon in 1917 [62]. He demonstrated that a 3D image of an unknown object could be reconstructed from an infinite number of projections of the object. In the case of CT, the acquisition is realized by rotating both the x-ray tube on one side and the detector on the opposite side of the patient in a synchronized way. In this case, the line integrals of the transmission of the x-ray beam through the object represent the projections that will serve to reconstruct the object. The reconstruction of images from the acquired projections is performed using the filtered backprojection algorithm.

One of the significant advantages of CT is that the reconstructed image scale, referred to as the Hounsfield unit (HU) scale, is linearly correlated with the linear attenuation coefficient of the corresponding biological tissue, thus giving direct physical information of the chemical composition of the tissues within the patient.

Magnetic Resonance Imaging (MRI)

This modality is sometimes also called Nuclear Magnetic Resonance Imaging (NMRI) because it uses the property of nuclear magnetic resonance of atoms inside the body. This is achieved by positioning the patient inside a strong magnetic field (B_0) used to align the magnetization of the protons of some atoms inside the body (related to the proton density). The application of a short radiofrequency (RF) pulse then produces an electromagnetic field with the resonance frequency just needed to tilt the global magnetization away from the magnetic field (B_0). When the pulse goes off, the magnetization re-aligns back to the magnetic field, producing a radio frequency signal that can be measured with receiver coils. The mechanisms of this relaxation, i.e. the longitudinal (T_1) and the transverse (T_2) relaxation times, are at the origin of this signal measurement. These relaxation times are the characteristics of different tissues and can be measured by applying suitable sequences of RF pulses to the region of interest and recording the radiofrequency NMR signals with a receiver coil.

Single-Photon Emission Computed Tomography (SPECT)

SPECT is a tomographic nuclear imaging technique enabling the generation of images representing the bio-distribution of gamma-ray emitting radiopharmaceuticals in the body acquired from standard planar emission projections around the patient. These images are usually obtained using one or more large scintillator detectors at the same time turning around the patient (180° or 360°), although new solid-state detector technologies dedicated for cardiac [26] and breast imaging [64] have recently been introduced in academic and corporate settings.

The reconstruction of images from the acquired projection data is usually performed by using either analytic algorithms (e.g. filtered backprojection, as in CT), or by the more popular iterative reconstruction methods which are now implemented on all commercial systems and widely used in practice [63]. Direct analytical techniques have the advantage of being straightforward and relatively fast but produce images with limited quality owing to the oversimplified line-integral model of the acquired projection data used. In contrast, iterative techniques are computationally more intensive but the resulting images are much improved (principally due to more accurate and complex modelling of the acquired projection data), which have enabled them to replace the analytic techniques.

Iterative algorithms involve a feedback process that allows a sequential tuning of the reconstruction to achieve a better match with the measured projection data. The iterative process starts with an initial estimate of the tracer distribution and calculates the corresponding projections using a forward projection operator incorporating an appropriate model of the emission and detection physics. Then, the difference between estimated and measured projections are be used to modify the original estimate of the tracer distribution through suitable additive or multiplicative corrections for each voxel using the backprojection operator. The adjusted tracer distribution then becomes the starting point for the next iteration and the process continues for a predetermined number of iterations using the continuous feedback loop until a final solution is reached.

Positron Emission Tomography (PET)

Similar to SPECT, PET is a nuclear medical imaging technique where a positron-emitting radiotracer is injected to the patient. ^{18}F-fluorodeoxyglucose (^{18}F-FDG), which is a glucose analogue, is the most widely used radiotracer in practice. Once a positron is emitted, it travels for a very short distance depending on its energy before annihilating with an electron to produce two anti-parallel annihilation photons each having an energy of 511 keV. The imaging procedure is based on the annihilation coincidence detection (ACD) of these two emitted photons. To achieve this, the patient is surrounded by a large number of detectors consisting of small scintillation crystals assembled in a cylindrical geometry. When both photons with energies of 511 keV are detected at the same time (with a time difference typically less than 500 ps, depending on the characteristics of the detectors), the event is accepted and the straight line joining these detectors defines a line of response (LoR).

The development of optimized detection geometries combined with high performance detector technologies and compact scanner design has become the goal of active research groups in both academic and corporate settings. Significant progress was achieved in the design of commercial PET instrumentation during the last decade allowing to reach a spatial resolution of about 4–6 mm for whole-body imaging, ~2.3 mm in PET cameras dedicated for brain imaging, and sub-millimeter resolution for female breast, prostate and small-animal imaging [16].

3 Basic Concepts of Image Quality

Assessing the quality of medical images is a very complex task. To understand the reasons for this complexity, one must keep in mind that the goal of medical imaging is not to produce pretty images but rather to provide non-invasive and informative diagnostic information that can help clinicians to make a diagnosis or to plan surgical or therapeutic procedures. The common problem is to determine the guidelines for an objective assessment of image quality by using established metrics [8].

The complexity of the whole process is shown in Fig. 10.1. The patient is usually referred for a medical imaging procedure to be carried out on a specific device depending on the clinical question. A plethora of structural and functional imaging techniques is available today. The collected information will usually be processed before it is displayed by a physical support, typically by a display monitor in a digitized facility or by conventional films in other modalities.

3.1 Image Contrast

The diagnostic accuracy and performance of the radiologist when reading these images was initially related to the concept of image quality [66]. The main factors influencing image quality are contrast, spatial resolution and noise. The contrast of an image can be defined as the difference (or in some cases the relative difference) between two neighbour signals coming from the object that is being imaged. For example:

- In projection radiography, this is the difference in x-ray transmission between two different structures, e.g. bone and soft tissue;
- In CT, this is related to the difference between the linear attenuation coefficients of two different tissues, e.g. soft tissue and fat;
- In PET, the difference is in the activity concentrations in two organs or tissues, i.e. normal and pathological tissues; and
- In MRI, the difference between the magnetic susceptibility of two tissues, e.g. white and gray matter in the brain.

3.2 Image Resolution

The spatial resolution is a measure of how close two adjacent objects can be distinguished. Usually, we express spatial resolution in units of spatial frequency, which is the inverse of the closest discrimination distance, or the number of sinusoidal cycles that can be fitted in unit space (cycles/mm). The spatial resolution

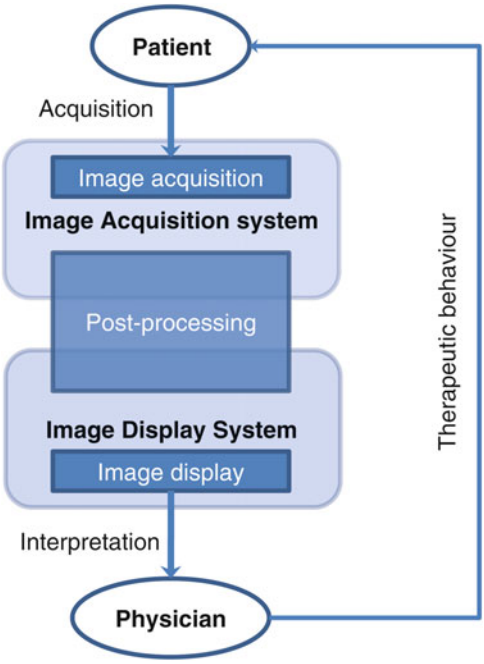

Fig. 10.1 Schema of diagnostic decision based on medical imaging acquisition and interpretation

is usually characterized by the modulation transfer function (MTF), which reports the amount of sinusoidal signals transferred by the imaging system (Fig. 10.2). This particular metric can be measured in analogue systems (e.g. screen-film) by sinusoidal test patterns using Coltman's method [18] or by using sharp-edge test phantoms on digital systems [68]. Alternatively, the analysis of the noise response can be used for this purpose [47].

3.3 Image Noise

Image noise is defined as the random variation of the signals. Since the imaging process is inherently statistical because of the nature of quantum physics, the noise is well described by Poisson/Gaussian functions. For this reason, the noise can simply be characterized as the standard deviation (σ) of the signal in a uniform region (Fig. 10.3). Nevertheless, this measure doesn't reflect the frequencial content of the noise which can be derived from the noise power spectrum (NPS) (Fig. 10.4), which in turn can be measured according to the International Electrotechnical Commission (IEC) standards (International Electrotechnical [39]).

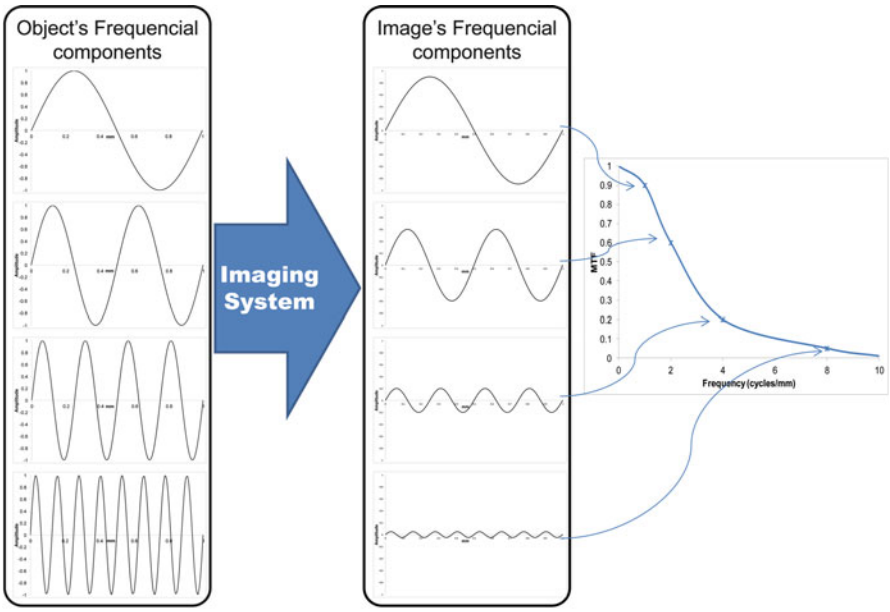

Fig. 10.2 Schema explaining the principle of modulation transfer function (*MTF*) measurement and its meaning. Four different frequential input signals (*left*), the signal output produced by the imaging system (*middle*) and the proportional restitution plotted as a function of spatial frequency.

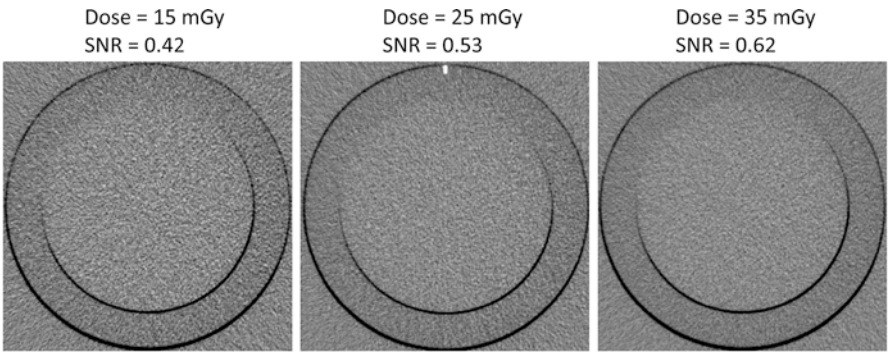

Fig. 10.3 CT images showing the effect of dose augmentation to noise and image quality. Uniform CT images with acquisition doses of 15, 25 and 35 mGy and their Signal to Noise Ratio (*SNR*). The signal is constant between these images because they are obtained from one unique object. However, the SNR improves by dose augmentation (from 15 to 35 mGy) due to a reduction of quantum noise

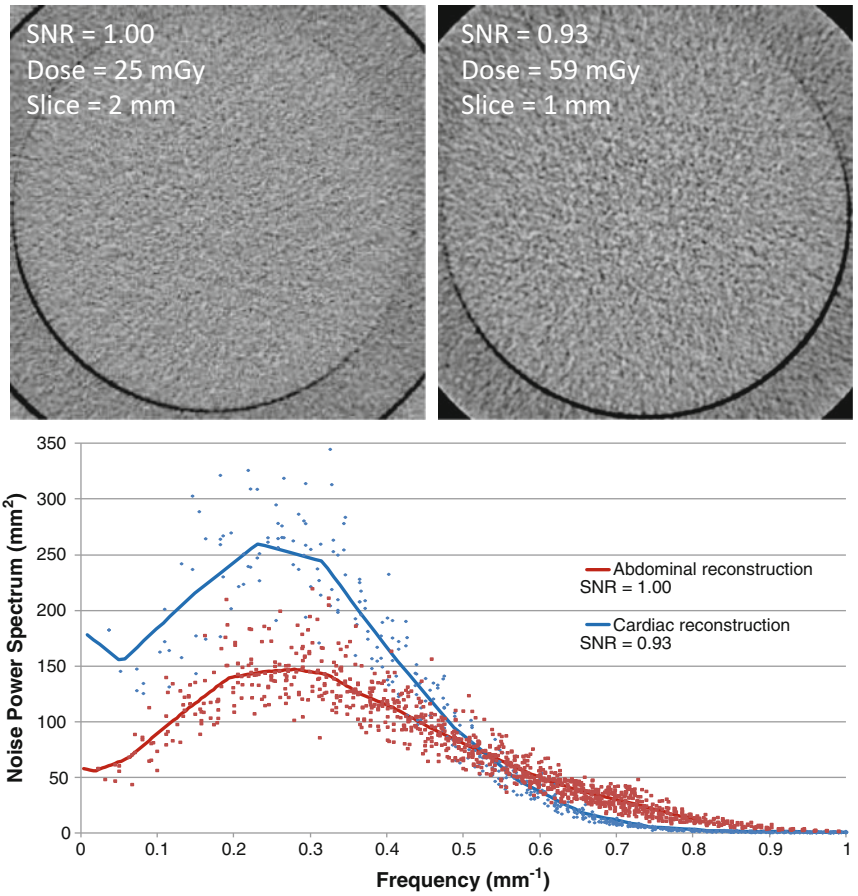

Fig. 10.4 CT images showing the effect of Weiner spectrum to noise and image quality. Uniform CT images with similar SNR meaning that both realisations contain the same magnitude of noise but different Weiner spectrum (also known as noise power spectrum), showing that the frequencial content of this noise is quite different

3.4 Signal Versus Noise

These image quality metrics described are closely linked and as such the interaction between them and the influence one has on others cannot be completely dissociated. For the task of image reading and interpretation by clinicians, other methods were proposed to better account for their imbrications. The limitations in terms of signal perception in noisy images was studied early in the Rose model [65] where the concept was extended to the so-called signal-to-noise ratio (SNR) (Fig. 10.3), which can be related to the probability of signal detection. The SNR can be defined as the difference in the mean output with (S_S) and without the signal (S_B) divided by the square root of the average variance of the noise, i.e. the standard deviation (σ):

$$SNR = \frac{S_s - S_B}{\sigma} = \frac{\Delta S}{\sigma}$$

This formalism was extended to new image quality assessment concepts that were introduced in the context of photographic imaging, such as detective quantum efficiency (*DQE*), which is a measure of the collective effects of the signal (associated with image contrast) and noise performance of an imaging system, usually expressed as a function of spatial frequency ω [21, 71]:

$$DQE(\omega) = \frac{SNR_{out}^2(\omega)}{SNR_{in}^2(\omega)}$$

where the SNR_{in} is the input *SNR* that originating from the object, or in other words, the *SNR* that will be achieved by an ideal detector, while SNR_{out} is the *SNR* that is obtained at the output of the imaging system. Obviously, all information should be obtained at the output of a perfect system, thus producing a *DQE* of 1, whereas a blind system will produce a *DQE* of 0.

One must keep in mind that the purpose of an image is to assist the observer (imaging specialist) in reaching a (clinical) decision. Therefore, image quality must be defined in terms of the targeted task [76]. Early contributions were made by Wagner for the task of discriminating between two different signals, i.e. present or absent, in the case of stationary Gaussian noise [75]. This task is commonly referred as the signal known exactly (*SKE*) and is used to introduce the concept of noise-equivalent quanta (*NEQ*), which depicts the minimum number of x-ray quanta necessary to generate a particular SNR by measuring change in the mean amplitude and in the variation in the amplitude of sine waves:

$$NEQ(\omega) = Q \cdot DQE(\omega)$$

where Q is the number of quanta incident on the detector that can be roughly equivalent to $SNR_{in}{}^2$, then:

$$NEQ(\omega) = \frac{|MTF(\omega)|^2}{NPS(\omega)}$$

The better the system performance, the higher the *NEQ* will be for all frequencies, while an *NEQ* of 0 means a blind system. As one can see, all the previous developments are closely related to statistical decision theory (SDT) that defines the framework where the *NEQ* was identified (*SKE*). This theory is based on the principle that any observer (human or mathematical) aiming at classifying an image (g) into one of two different categories, i.e. positive or negative, will perform this task through a statistical calculation (λ) to be compared with a threshold λ_0 that defines if the image belongs to any of the previously defined categories (Fig. 10.5).

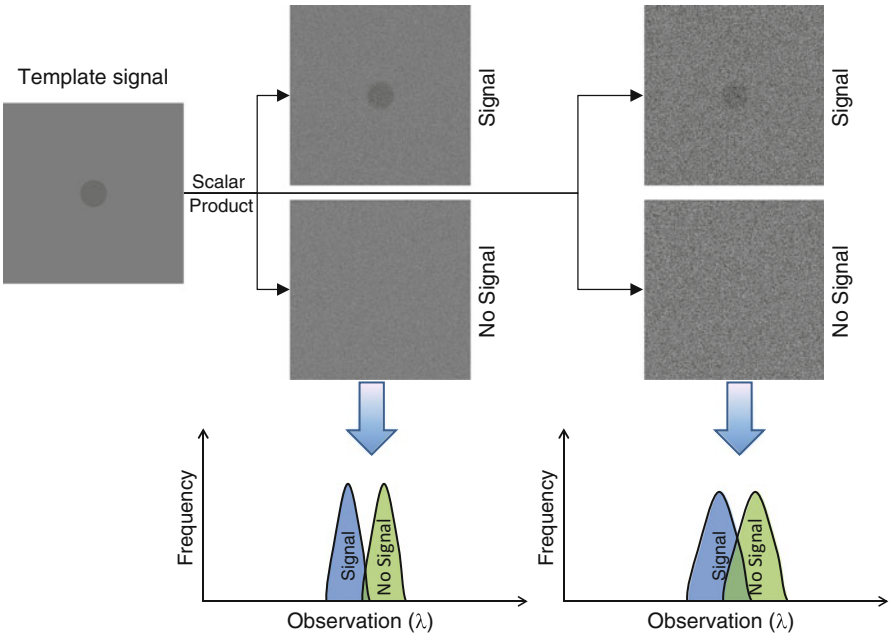

Fig. 10.5 Simple schema of the linear observer model principle. A template signal is compared (scalar product) with different noise realizations of signal-present and signal-absent images to produce task-dependent figures of merit that allow the discrimination between signal-present and signal-absent situations

If the decision is positive, the hope is that it is correct (True Positive: TP), but there are chances that the decision is wrong (False Positive: FP). The same could happen if the decision is negative (TN and FN, respectively). The compromise between the TP rate (TPR: Sensitivity) and the FP rate (FPR: 1 – Specificity) is defined by the decision threshold λ_0, and the variation of this threshold leads to the construction of the receiver operating curve (ROC) [54, 55], whose area under the curve (AUC) can be adopted as a image quality criteria (Fig. 10.6). For particular conditions, this metric can be related to a discrimination task [27] and as a consequence to the SNR. The AUC can change from 0.5 (random choice) to 1 (perfect performance) but its shape can be the sign of a highly sensitive or highly specific imaging system.

As stated earlier, the observer in the SDT can be mathematical, i.e. observer models. The most widely used are the linear observer models because the statistical calculation (λ) is a vectorial product of the image (g) and a discriminant function (u). Different variations of this model and optimal choice of the discriminant function are described elsewhere [9].

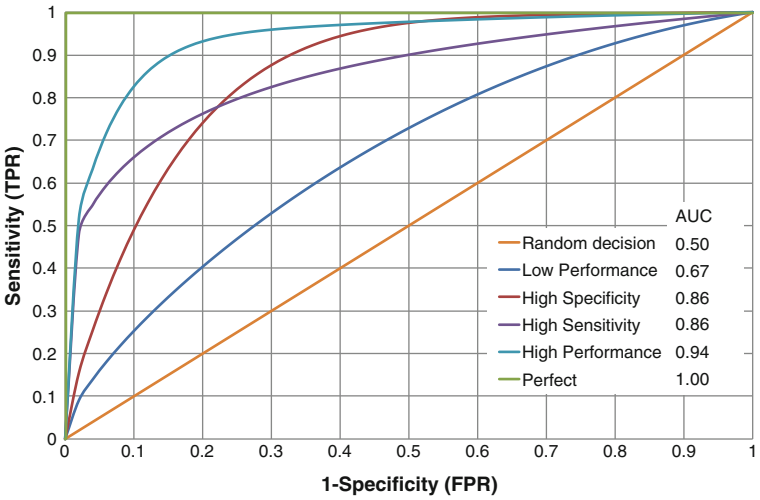

Fig. 10.6 Receiver Operating Curve (*ROC*) analysis as a metric in the statistical decision theory

4 Dose Reduction Strategies

To understand the magnitude of radiation exposure arising from medical imaging procedure, national surveys were carried out by different bodies in various countries worldwide. For instance, the National Radiological Protection Board (NRPB) performed periodic surveys of medical imaging practice in the UK to gauge individual and collective radiation doses. It has been shown in the NRPB-W4 report [30] that conventional radiography accounts for about 90 % of the total procedures and represents about 38 % of the collective dose. While mammography accounts for approximately 4 % of the total x-ray procedures, it represents roughly 2.4 % of the collective dose. Fluoroscopy represents just about 1.5 % of the total procedures but accounts for 16 % of the collective dose. For the latter, radiation protection is an important issue for the medical staff because this technique is widely used in interventional radiology.

CT has opened new opportunities in medical imaging in the last 40 years, but it has become a major source of medical exposure as it represents almost 40 % of the collective dose [30] despite accounting for only 3.3 % of the total procedures using ionizing radiation. The issue is that the frequency of CT procedures is still growing and recently became a public health concern for different governments [72], thus indicating that despite much worthwhile efforts targeting dose optimisation in CT, the topic still requires further research and development.

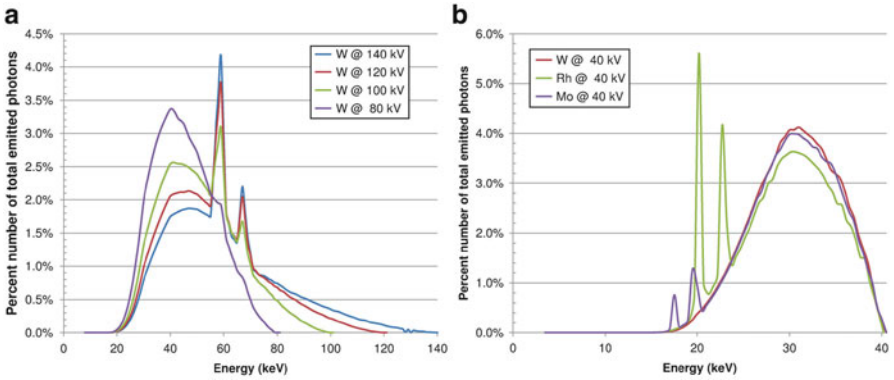

Fig. 10.7 Emitted x-ray spectra for different voltages and anodes. (**a**) Spectrum of Tungsten (*W*) anode x-ray tube for voltages of 80, 100, 120 and 140 kV. (**b**) Spectrum of x-ray tube voltages of 40 kV with anodes of Tungsten (*W*), Rhodium (*Rh*) and Molybdenum (*Mo*)

4.1 Hardware Innovations

Since projection radiography was the first introduced radiographic imaging technique, related technological advances are enormous. The first advance in technology was made by adapting the x-ray beam spectrum to energy changes (Fig. 10.7a). This allows the user to choose an optimal spectrum depending on the required procedure. For example, in chest radiography, higher energies (100–120 kV) are used because low contrast imaging between lungs and bones is desirable. On the opposite, low energy beams are used, for example, in orthopaedic radiography where high contrast between bones and soft tissue is needed. A big advance in x-ray tube design was achieved following the introduction of special dedicated mammographic anodes (molybdenum anodes) in 1965 (Fig. 10.7b). This was followed by rhodium anodes and filtrations made with the same material. These specific anodes present a high emission probability of two particular energies (characteristic radiation) at 17.9 and 19.5 keV for molybdenum, which are optimum to obtain very good contrast with smaller breast; while rhodium anodes have characteristic radiation at 20.3 and 22.7 keV, which are optimal for larger breasts, making it possible to save up to 40 % of the dose specially for larger breasts [45].

Detector technologies for projection imaging started with photographic film-based detectors that were subsequently improved following the introduction of fluorescent screens (analogue). The contrast capability of these detectors was defined by the characteristic curve [36], which measures how the film opacity (most precisely the log of the opacity) changes as a function of the log of the x-ray exposure. The higher the difference in the opacity for a smaller exposure, the higher is the contrast capability of the film. An example of such a curve is shown in Fig. 10.8, demonstrating the associated gradient of the curve calculated at each measurement point, which is representative of the film contrast.

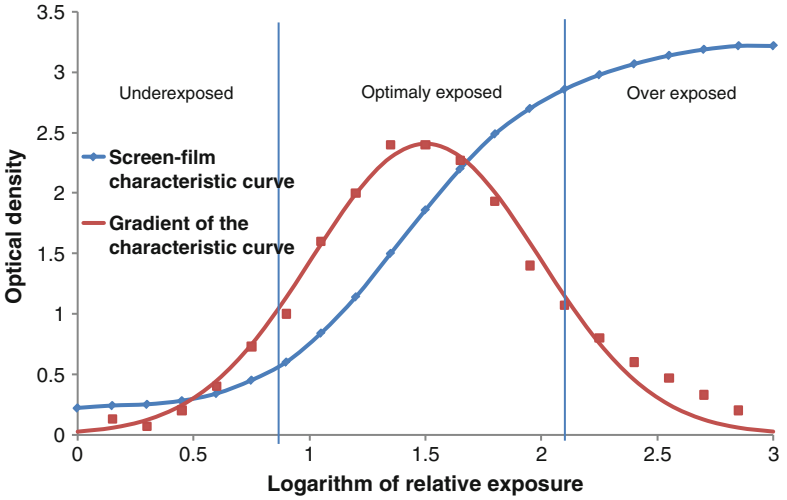

Fig. 10.8 Screen-film exposure characteristic curve

One can see that this curve has an "S" shape on the left and right sides (respectively underexposed and overexposed regions). Both regions are flat owing to the small contrast capability also put into evidence by the lower values on the gradient curve, while the central part (optimal exposition) shows a better contrast capability. For this reason, patient exposure is directly related to the type of screen-film employed since the exposure must be very close to the central part of this curve.

As a matter of fact, optimal exposure of films proved to be a difficult task to achieve given that the operator has to be consistent for different procedures to avoid errors. As a consequence, the concept of automatic exposure control (AEC) was developed with the aim to optimize the exposure of films under different settings [58]. At the present time, the technology changed to digital detectors where the contrast is no more dependent on the exposure (almost linear) as shown on the characteristic curve of two different detectors (Fig. 10.9). However, this remains a challenging issue when setting-up AEC devices [42]. Nevertheless, when these detectors were introduced, their performance was not optimal and as such their limited spatial resolution reduced their *NEQ* and *DQE* [57]. Recent advances in detector design overcome this drawback and result in better performance [56].

CT is a high dose procedure. Paradoxically the technical advances that allowed significant improvement in image quality were responsible for the increasing use of this technology by opening new avenues and offering novel diagnostic applications. The first CT scanner was built in 1972. It was first used to scan a brain inserted in a water-box at a speed of 4 min per rotation and required overnight reconstruction of the 8 mm thick images. The first waterless whole body scanner was developed in 1974 [48]. Given the slow acquisition time, motion blurring was an important limitation in terms of spatial resolution degradation. This was significantly reduced

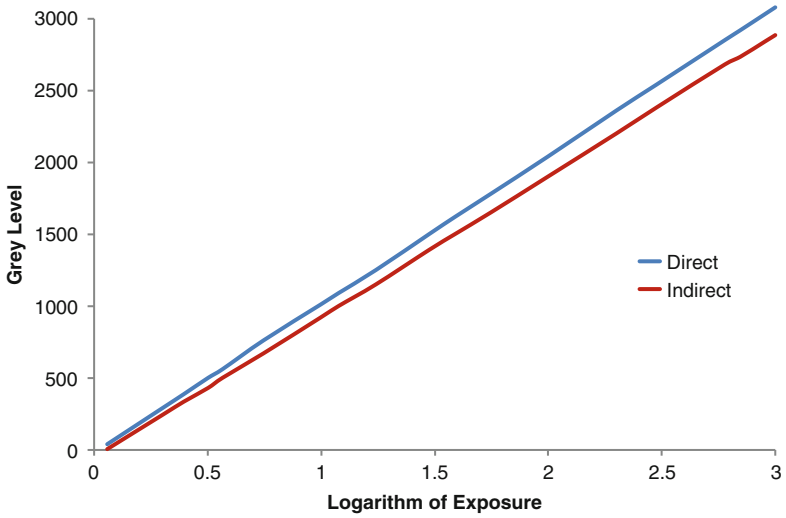

Fig. 10.9 Digital detectors exposure characteristic curve

by the introduction of the second-generation CT scanners through the use of narrow beams (contrary to its single-beam progenitor) and multiple detectors (3 in the beginning) that reduced motion blur by increasing rotation speed to 20 s per rotation. This idea was further exploited in the third generation CT scanners by introducing fan beams that cover the patient's width and by applying an array of detectors (250 to 750) to capture the entire beam, thus increasing the rotation speed. This was made possible by the introduction of high performance proportional detectors (e.g. Xenon detectors) that do not require recalibration prior to scanning [12] to enable axial translation (1st and 2nd generation scanners). This last advancement was crucial for the design of third generation scanners without axial translation, defining the basic geometry of current CT scanners (Fig. 10.10).

The slip ring technology was the next major advance in CT, allowing a continuous rotation of the x-ray tube/detector gantry, and was subsequently consolidated with helical scanning to reduce the acquisition time to about 1 s [41]. The helical pitch concept, defined as the table movement per rotation divided by the slice thickness, was also introduced with this technology. This allowed dose reduction when the pitch is higher than 1 by avoiding the irradiation of a smaller surface of the patient, but compromising image quality to some extent since the reconstruction is performed with interpolation of the missing data.

Another major leap in CT technology was the introduction of dual-slice scanning that opened the door to multi-slice CT scanners, thus enabling larger axial coverage per tube rotation. The consequence is faster acquisition without noticeable impact on individual patient dose [74]. Current technology permits acquisitions of up to 320-slices [70], with sub-millimetric slice thickness and rotation time of less than half a second.

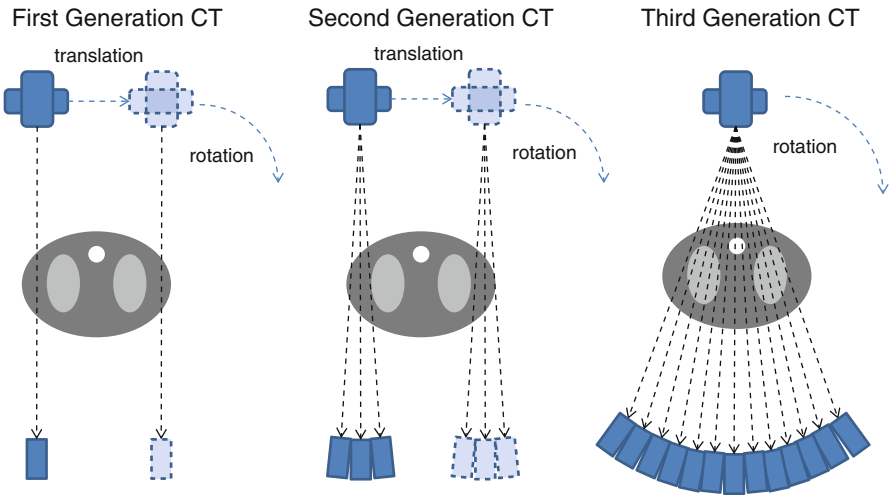

Fig. 10.10 Evolution of CT scanner acquisition techniques

With respect to dose reduction strategies, beam hardening filters have long been employed in x-ray CT to preferentially absorb soft and low-energy x-rays, which have little or no contribution to image formation, thus allowing the reduction of patient dose and beam hardening artefacts [5]. The introduction of AEC devices proved to be clinically relevant and had a significant impact in clinical practice (Fig. 10.11). The principle of AEC is to modulate the tube current as a function of patient attenuation during table movement (z-modulation) and also during the x-ray tube rotation (xy-modulation). The user can lever this modulation by choosing either a noise index or a reference tube current that will produce a preset noise level. The results have demonstrated that dose saving can be effective provided the scanner is used by a well-trained operator. This last observation, even if obvious and fundamental, is not so easy to implement in practice, since CT protocols must be adapted to new AEC devices. The motivations behind improvement in image quality are legitimate; however, the radiologist must keep in mind that the goal of imaging is to achieve clinical diagnosis and not simply to produce pretty images. Part of the responsibility can be attributed to scanner manufacturers who must train the end users to optimize the use of these devices. To avoid potential problems, the choice of noise reference level must be realistic and a maximum current exposure threshold must be set to avoid excessive exposure to patients, particularly in large and obese subjects [29, 52].

New research directions were explored during the last decade including dual-source CT (DSCT) [22–24] to achieve much better contrast discrimination and to improve spatial and temporal resolution. Increasing radiation dose remains the major concern. Even if an individual dose is not significantly increased, the increasing demand and utilization generated by improved image quality and increase applications will lead to a significant increase in the collective dose.

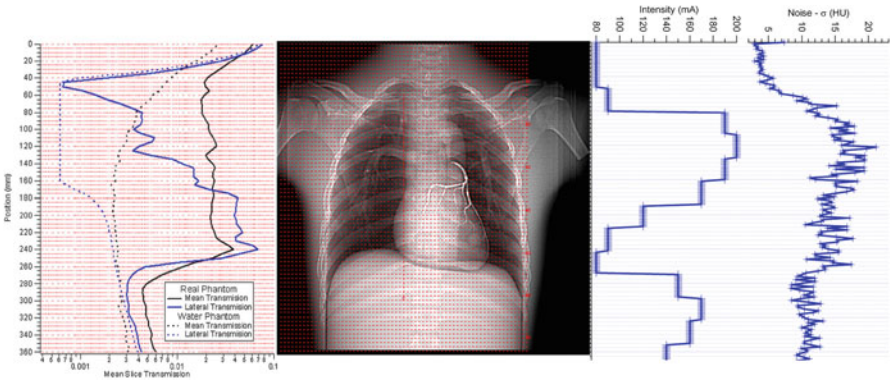

Fig. 10.11 Schema explaining the principle of automatic exposure control (*AEC*). *Left*: mean slice and lateral transmisions obtained with the experimental set-up (*continuous line*) and calculated with the hypothesis of a phantom having the same shape but filled with water (*dashed line*) showing the shape-only transmision dependency. *Middle left*: Topogram of the phantom. *Middle right*: Current intensity modulation obtained with AEC, very similar to the shape-only transmision curve. *Right*: The resulted mean noise with AEC, which should be as constant as possible

On the other hand, nuclear medicine forms a special category of medical imaging techniques in the sense that the information provided is functional rather than anatomical. The contrast and image quality reflecting tracer biodistribution in different tissues and organs are subjected to high statistical uncertainty given the small activity administered to the patient. For this reason, the performance of an imaging device is highly dependent on its sensitivity, which is defined as the number of counts detected per unit time per unit of activity present in the body region being studied [13]. The sensitivity depends on many parameters including geometric efficiency, crystal detection efficiency ... etc. In the early days of PET imaging, detectors were made of thallium-doped sodium iodide (NaI[Tl]) crystals similar to Anger cameras used for SPECT imaging. This technology was first replaced by Bismuth Germinate (BGO) crystals ($Bi_4Ge_3O_{12}$) introduced in 1973 [79], chosen mainly because of its higher efficiency at 511 keV. Gadolinium Oxyorthosilicate (GSO) (Gd_2SiO_5) is another popular scintillator used on commercial PET scanners [33], but the current materials of choice are Lutetium Oxyorthosilicate (LSO) crystals (Lu_2SiO_5) [53] and Cerium-doped Lutetium Yttrium Orthosilicate (LYSO) crytals ($Lu_{2(1-x)}Y_{2x}SiO_5$:Ce).

The availability of faster scintillation crystals and electronics renewed an interest in old technologies such as time-of-flight (ToF) PET and made this approach feasible on commercial clinical systems. First attempts relied on crystals such as Barium Fluoride (BaF_2) because of its very good time resolution of 156 picoseconds (ps) [4, 49]. Time-of-flight exploits the difference in the arrival time between the two crystals in coincidence to reduce the uncertainty in the annihilation point of the coincidence event to a limited region along the line of response, thus substantially diminish the noise in the reconstructed images. A timing resolution of 500 ps results in a reduction of a factor of five in the variance of the reconstructed image

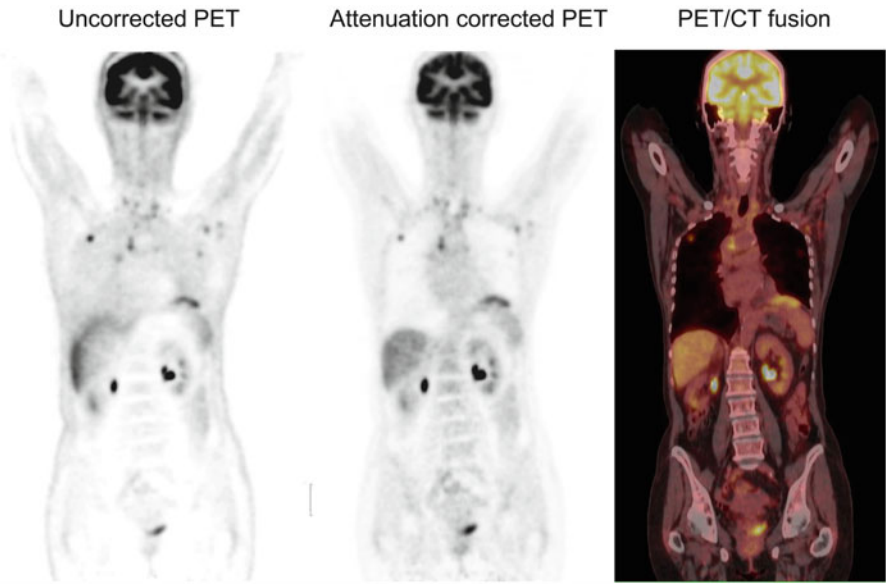

Fig. 10.12 Coronal PET images with and without CT-based attenuation correction and a fused PET/CT image. *Left*: Uncorrected PET image showing an underestimation of tracer uptake in the central part of the image. *Middle*: attenuation corrected PET image with the map derived from the corresponding CT image. *Right*: Fused PET and CT image putting into perspective complementary functional (*PET*) and anatomical (*CT*) information

compared to conventional PET [59]. It has been demonstrated that ToF-PET enables a much better compromise between contrast and noise, a property that is most invaluable in challenging situations such as: low statistic studies, scans requiring short examination time, large patients, low uptake . . .etc. [19]. This technical innovation increases throughput, improves patient comfort, and reduces the patient dose by lowering the administered dose without deteriorating image quality. The administered activity of PET tracers could be tailored to an individual through the use of appropriate metrics reflecting data quality, such as noise-equivalent counting rate (NECR). It has been shown that the clinical NECR response matching individual patient scans can be accurately modelled to optimize the activity to be administered to an individual, thus reducing patient dose [77].

The introduction of dual-modality PET/CT imaging systems in clinical environments has revolutionized the practice of medical imaging [73]. The complementarity between the detailed anatomical (CT) and functional or metabolic (PET) information provided in a "one-stop shop" and the possibility of using CT images for attenuation correction of the PET data has been the driving force behind the success of this technology. Photon attenuation in the body during data acquisition is an important source of image degradation in PET. Despite the non-negligible increase in radiation dose [35, 84], the use of CT-based attenuation compensation has many advantages compared to conventional transmission-based scanning and

has received a great deal of attention in the literature [46, 86]. Various dose reduction strategies including the use of low-dose CT protocols are becoming available for clinic use [80]. Attenuation correction is now recognized as an important image correction procedure not only for accurate quantification of PET images but also for lesion detection and accurate localization [6] (Fig. 10.12). Dedicated paediatric PET/CT protocols were developed to shorten acquisition time and reduce dose [1, 3].

Following the trend of hybrid PET/CT, PET/MR was introduced into clinical practice and is progressively becoming recognized by the medical community [25, 69]. MRI and PET offer complementary sensitivity and functional data respectively. When these technologies are combined together into a system that is capable of simultaneous acquisition will capitalize the strengths of each other [61]. The most important advantages of hybrid PET/MR technology in that anatomical MRI provides better soft tissue contrast compared to CT and this contrast can be adapted through the use of various sequences [85]. MR can also provide significant functional data of its own, such as diffusion-weighted MR for assessing tissue ischemia, contrast-based perfusion measurements in the brain and heart, fMRI and angiography. In addition, in contrast to CT, MRI does not use ionizing radiation and as such, it has major advantages when dose reduction is a concern, e.g. in paediatric application. Nevertheless, some general guidelines highlighting the major concerns for this imaging modality were developed for the users [37, 38]. These mostly emanate from the high-gradient fields that can stimulate some nerves and produce a sensation of discomfort and pain, particularly for those individuals taking drugs or afflicted with epilepsy. RF pulses can also induce heating of biological tissues.

There are several ways to combine PET and MRI data of the same patient [85]. The most straightforward approach is to adopt the configuration of PET/CT, in the so-called "tandem" arrangement, where the two procedures are performed sequentially in space and time. However, a very attractive solution is to acquire MRI and PET data simultaneously in space and probably in time. This innovative approach has resulted firstly in the design of an "insert" concept, where a small axial size MR-compatible PET insert fits inside a standard MRI scanner, and secondly to a completely integrated version, where a dedicated whole body PET scanner is built within a dedicated MRI scanner. This latter conceptual design is the most attractive but also the most challenging to achieve. However, it is certainly the way forward to optimize the use of combined PET/MRI systems in clinical diagnosis, therapy and follow-up.

Similar to PET/CT, the anatomical information from MRI can be useful for many other tasks including attenuation compensation, transmission-based scatter modelling, motion detection and correction, partial volume correction, and introducing *a priori* anatomical information into the reconstruction of the PET emission data. Given its clinical relevance and the challenges, the development of robust strategies for MRI-guided attenuation correction remains a major drawback and will probably be solved by strengthening research and developing innovative solutions in this area [32, 83].

With the advent of full digital systems, image display must be also ensure a high quality display of medical images by respecting well established standards of

reliability. Different standards were proposed but the most widely used are those detailed in the German DIN 6868–57 regulation [20] and its US counterpart published in the AAPM TG18 report [67]. While most of the requirements of these standards are fulfilled by all commercial systems, the most important one is the greyscale display conformance with the DICOM 3.14 standard, which is the most difficult to comply since not all monitors (especially common desktop display systems) conform to this requirement [28]. Special attention should therefore be paid to this issue since it might compromise the whole medical imaging chain.

4.2 Software Innovations

In parallel to hardware solutions to reduce patient dose without sacrificing image quality, software approaches were developed to achieve this goal mostly through the use of advanced image processing to enhance image quality or innovative image reconstruction strategies in emission and transmission tomography to reduce the high noise typically present in low-dose scanning protocols. The reduction of image noise and streak artefact in low dose CT scans using specially designed noise reduction filters successfully achieved this goal at the expense of image sharpness and contrast as well as slightly altered modulation transfer function at higher spatial frequencies. Various filters have been suggested in the literature with varying degrees of success. Filtering can be performed either in image space [43] or projection space [40]. The latter has some advantages in terms of spatial resolution loss, which is important in clinical diagnosis.

Alternative techniques were suggested to deal with the challenging task of streak artefacts removal given the difficulty of discriminating them from the attenuation information of biologic tissues. One such technique, referred to as artefact suppressed large-scale nonlocal means, consists of a two-step processing scheme for suppressing both noise and artefacts in thoracic LDCT images. The idea is to exploit the specific scale and direction properties to discriminate noise and artefacts from the imaged structures [15].

On the other hand, the introduction and widespread commercial adoption of iterative reconstruction techniques in emission tomography spurred renewed interest in their use in other imaging modalities including x-ray CT. Basically, two major classes of image reconstruction algorithms are used in CT: direct analytical methods and iterative methods. Until recently, the most widely used methods for image reconstruction were direct analytical techniques because they are relatively quick and their derivation straightforward. However, the resulting image quality is limited by the over simplified line-integral model of the acquired projection data. In contrast, iterative techniques are computationally more intensive but the resulting images demonstrate improvements (principally arising from more accurate modelling of the acquired projection data) which have enabled them to replace analytic techniques not only in research but also in clinical settings [60].

Iterative reconstruction techniques came forward in x-ray CT after having been abandoned owing to the large amount of data produced by the latest generation of CT scanners and the associated computational burden. The widespread availability of high performance computing even on desktop computers (including GPU and cloud computing), and the continuing endeavours towards dose reduction in diagnostic procedures led to renewed interest in iterative techniques and made them a hot topic for the leading manufacturers of clinical CT scanners.

Iterative techniques are commonly used in problems that involve optimization. The reconstruction problem can be considered a particular case where one is trying to determine the 'best' estimate of the distribution of attenuation coefficients in CT based on the measured projections (sinograms). Iterative reconstruction has a number of impending advantages that make it attractive in comparison with conventional analytical reconstruction methods. Foremost is the limiting assumption in analytical techniques that the measured projection data are perfectly consistent with the object to be reconstructed, a requirement that is certainly not exact in practice given the presence of noise and other physical factors (e.g. beam hardening, scatter, detector spatial response, truncation ... etc.). Iterative algorithms are well suited to handling complex physical models of the transmission and detection processes. This ability to directly model the system response, including some consideration of the noise characteristics, provides substantial flexibility in the type of data that can be reconstructed.

The popularity of iterative image reconstruction stems from substantial improvement of image quality, particularly for low-dose protocols [10]. Most manufacturers have recently implemented iterative reconstruction techniques into their platforms, thus enabling the use of ultra-low dose protocols without sacrificing image quality [44, 51, 81]. As such, substantial reduction in patient dose (in the range 40–80 %) could be achieved using this class of reconstruction algorithms. It is expected that iterative CT reconstruction implemented on commercial cloud computing environments will be available in the near future.

Computer-aided diagnosis (CAD) has been one of the major research topics in medical imaging and diagnostic radiology. As such, it has become an integral part of routine clinical workflow for the detection of breast cancer by mammography at many screening facilities. However, the technique is still in its infancy given the enormous potential expected for its application to the detection of other diseases based on analysis performed on various single and hybrid imaging modalities.

5 Summary

Over the past three decades, we have witnessed significant advances in medical imaging, which have revolutionized the assessment of a multitude of disorders with high accuracy and precise spatial resolution. Recent advances in medical imaging system design have resulted in significant improvements in anatomical, functional, and dynamic imaging procedures taking advantage of innovative approaches in

image reconstruction and analysis strategies. With these developments, computer-aided diagnosis is becoming a reality. These computer-based tools allow physicians to understand and diagnose disease through virtual interaction. The role of medical imaging is not limited to the visualization and evaluation of structure and function, but goes beyond that to diagnosis, surgical planning, simulation, and radiotherapy planning.

Better communication and collaboration between the end-users and equipment vendors in research (by providing feedback) and better clinical utilization (through better commissioning, quality assurance, education and training, developing standards and implementing policies) improves daily practice and the optimization of radiation protection. Senior leadership teams can inspire and encourage other individuals, team members and health care organizations to change, adapt, grow, and prepare for the future challenges. This can be achieved through creative dialogue between multidisciplinary teams, thus facilitating a culture of best practice, and providing the necessary skills to better-prepare future medical imaging leaders. With the ever-increasing costs and challenges in health care, there is a strong need for innovative leaders to develop new models for the healthcare systems where medical imaging plays a pivotal role.

On reflection, it is gratifying to witness the vast progress that multimodality imaging has made in the last two decades through leadership and innovation in the various disciplines. It is expected that with the availability of high-resolution multimodality imaging systems in the near future, molecular imaging-based and personalized medicine will become clinically feasible.

Acknowledgements This work was supported by the Swiss National Science Foundation under grant SNSF 31003A-135576, Geneva Cancer League, the Indo-Swiss Joint Research Programme ISJRP 138866, and Geneva University Hospital under grant PRD 11-II-1.

References

1. Accorsi R, Karp JS, Surti S (2010) Improved dose regimen in pediatric PET. J Nucl Med 51(2):293–300
2. Alavi A, Basu S, Torigian D et al (2008) Is planar imaging in radiology and nuclear medicine a viable option for the 21st century? Q J Nucl Med Mol Imaging 52(4):319–322
3. Alessio AM, Kinahan PE, Manchanda V et al (2009) Weight-based, low-dose pediatric whole-body PET/CT protocols. J Nucl Med 50(10):1570–1577
4. Allemand R, Gresset C, Vacher J (1980) Potential advantages of a cesium fluoride scintillator for a time-of-flight positron camera. J Nucl Med 21(2):153–155
5. Ay MR, Mehranian A, Maleki A, Ghadiri H, Ghafarian P, Zaidi H (2013) Experimental assessment of the influence of beam hardening filters on image quality and patient dose in volumetric 64-slice x-ray CT scanners. Phys Medica 29(3):249–260
6. Bai C, Kinahan PE, Brasse D et al (2003) An analytic study of the effects of attenuation on tumor detection in whole-body PET oncology imaging. J Nucl Med 44(11):1855–1861
7. Ballinger J (2008) Re: planar and SPECT imaging in the era of PET and PET-CT: can it survive the test of time? Eur J Nucl Med Mol Imaging 35(12):2340

8. Barrett HH, Myers KJ (2003) Foundations of image science. Wiley, New Jersey
9. Barrett HH, Yao J, Rolland JP et al (1993) Model observers for assessment of image quality. Proc Natl Acad Sci U S A 90(21):9758–9765
10. Beister M, Kolditz D, Kalender WA (2012) Iterative reconstruction methods in X-ray CT. Phys Med 28(2):94–108
11. Bonte FJ (1976) Nuclear Medicine Pioneer Citation, 1976: David E Kuhl MD. J Nucl Med 17(6):518–519
12. Boyd D, Coonrod J, Dehnert J et al (1974) A high pressure xenon proportional chamber for x-ray laminographic reconstruction using fan beam geometry. IEEE Trans Nucl Sci 21:184–187
13. Budinger TF (1998) PET instrumentation: what are the limits? Semin Nucl Med 28(3):247–267
14. Bushberg JT, Seibert JA, Leidholdt EM (2002) The essential physics of medical imaging, 2nd edn. Lippincott Williams & Wilkins, Philadelphia
15. Chen Y, Yang Z, Hu Y et al (2012) Thoracic low-dose CT image processing using an artifact suppressed large-scale nonlocal means. Phys Med Biol 57(9):2667–2688
16. Cherry SR (2006) The 2006 Henry N. Wagner lecture: of mice and men (and positrons) -advances in PET imaging technology. J Nucl Med 47(11):1735–1745
17. Cherry SR, Sorenson JA, Phelps ME (2004) Physics in nuclear medicine, 3rd edn. Elsevier Health Sciences, Philadelphia
18. Coltman JW (1954) The specification of imaging properties by response to a sine wave. J Opt Soc Am 44:468–469
19. Conti M (2011) Focus on time-of-flight PET: the benefits of improved time resolution. Eur J Nucl Med Mol Imaging 38(6):1147–1157
20. Deutsches Institut für Normung (2012) Publication DIN 6868–157 Image quality assurance in diagnostic X-ray departments – Part 157: RöV acceptance and constancy test of image display systems in theirs environment. Deutsches Institut für Normung, Berlin
21. Fellgett BP (1958) Equivalent quantum-efficiencies of photographic emulsions. The Observatories, Cambridge
22. Flohr TG, Bruder H, Stierstorfer K et al (2008) Image reconstruction and image quality evaluation for a dual source CT scanner. Med Phys 35(12):5882–5897
23. Flohr TG, Leng S, Yu L et al (2009) Dual-source spiral CT with pitch up to 3.2 and 75 ms temporal resolution: image reconstruction and assessment of image quality. Med Phys 36 (12):5641–5653
24. Flohr TG, McCollough CH, Bruder H et al (2006) First performance evaluation of a dual-source CT (DSCT) system. Eur Radiol 16(2):256–268
25. Gaa J, Rummeny EJ, Seemann MD (2004) Whole-body imaging with PET/MRI. Eur J Med Res 9(6):309–312
26. Gambhir SS, Berman DS, Ziffer J et al (2009) A novel high-sensitivity rapid-acquisition single-photon cardiac imaging camera. J Nucl Med 50(4):635–643
27. Green DM, Swets JA (1974) Signal detection theory and psychophysics. Krieger Publishing, New York
28. Gutierrez D, Monnin P, Valley JF et al (2005) A strategy to qualify the performance of radiographic monitors. Radiat Prot Dosimetry 114(1–3):192–197
29. Gutierrez D, Schmidt S, Denys A et al (2007) CT-automatic exposure control devices: what are their performances? Nucl Instrum Methods Phys Res A 580:990–995
30. Hart D, Wall BF (2002) Radiation exposure of the UK population from medical and dental X-ray examinations. Publication NRPB-W4. National Radiological Protection Board, Chilton
31. Hasegawa B, Zaidi H (2006) Dual-modality imaging: more than the sum of its components. In: Zaidi H (ed) Quantitative analysis in nuclear medicine imaging. Springer, New York
32. Hofmann M, Pichler B, Schölkopf B et al (2009) Towards quantitative PET/MRI: a review of MR-based attenuation correction techniques. Eur J Nucl Med Mol Imaging 36(Suppl 1):93–104

33. Holte S, Ostertag H, Kesselberg M (1987) A preliminary evaluation of a dual crystal positron camera. J Comput Assist Tomogr 11(4):691–697
34. Hounsfield GN (1973) Computerized transverse axial scanning (tomography) 1. Description of system. Br J Radiol 46(552):1016–1022
35. Huang B, Law MW, Khong PL (2009) Whole-body PET/CT scanning: estimation of radiation dose and cancer risk. Radiology 251(1):166–174
36. Hurter F, Driffield VC (1890) Photochemical investigations and a new method of determination of the sensitiveness of photographic plates. J Soc Chem Indian 9:455
37. International Commission on Non-Ionizing Radiation Protection (1998) Guidelines for limiting exposure to time-varying electric, magnetic, and electromagnetic fields (up to 300 GHz). Health Phys 74(4):494–522
38. International Commission on Non-Ionizing Radiation Protection (2004) Medical magnetic resonance (MR) procedures: protection of patients. Health Phys 87(2):197–216
39. International Electrotechnical Commission (2003) Medical electrical equipment – characteristics of digital X-ray imaging devices. Part 1: determination of the detective quantum efficiency. International Electrotechnical Commission, Geneva, 62220–1
40. Kachelriess M, Watzke O, Kalender WA (2001) Generalized multi-dimensional adaptive filtering for conventional and spiral single-slice, multi-slice, and cone-beam CT. Med Phys 28(4):475–490
41. Kalender WA, Seissler W, Klotz E et al (1990) Spiral volumetric CT with single-breath-hold technique, continuous transport, and continuous scanner rotation. Radiology 176(1):181–183
42. Kalra MK, Maher MM, Toth TL et al (2004) Techniques and applications of automatic tube current modulation for CT. Radiology 233(3):649–657
43. Kalra MK, Wittram C, Maher MM et al (2003) Can noise reduction filters improve low-radiation-dose chest CT images? Pilot study. Radiology 228(1):257–264
44. Katsura M, Matsuda I, Akahane M et al (2012) Model-based iterative reconstruction technique for radiation dose reduction in chest CT: comparison with the adaptive statistical iterative reconstruction technique. Eur Radiol 22(8):1613–1623
45. Kimme-Smith C, Wang J, DeBruhl N et al (1994) Mammograms obtained with rhodium vs molybdenum anodes: contrast and dose differences. AJR Am J Roentgenol 162(6): 1313–1317
46. Kinahan PE, Hasegawa BH, Beyer T (2003) X-ray-based attenuation correction for positron emission tomography/computed tomography scanners. Semin Nucl Med 33(3):166–179
47. Kuhls-Gilcrist A, Jain A, Bednarek DR et al (2010) Accurate MTF measurement in digital radiography using noise response. Med Phys 37(2):724–735
48. Lcdley RS, Chiro GD, Luessenhop AJ et al (1974) Computerized transaxial X-ray tomography of the human body. Science 186:207–212
49. Lewellen TK (1998) Time-of-flight PET. Semin Nucl Med 28(3):268–275
50. Mariani G, Bruselli L, Duatti A et al (2008) Is PET always an advantage versus planar and SPECT imaging? Eur J Nucl Med Mol Imaging 35(8):1560–1565
51. Marin D, Nelson RC, Schindera ST et al (2010) Low-tube-voltage, high-tube-current multidetector abdominal CT: improved image quality and decreased radiation dose with adaptive statistical iterative reconstruction algorithm-initial clinical experience. Radiology 254(1):145–153
52. Matsumoto Y, Masuda T, Imada N et al (2012) Examination of the chest computed tomography scan condition optimization in consideration of the influence of the position of the arms. Nihon Hoshasen Gijutsu Gakkai Zasshi 68(7):851–856
53. Melcher CL, Schweitzer JS (1992) Cerium-doped lutetium oxyorthosilicate: a fast, efficient new scintillator. IEEE Trans Nucl Sci 39:502–505
54. Metz C (2008) ROC analysis in medical imaging: a tutorial review of the literature. Radiol Phys Technol 1(1):2–12
55. Metz CE (1986) ROC methodology in radiologic imaging. Invest Radiol 21(9):720–733
56. Monnin P, Gutierrez D, Bulling S et al (2007) A comparison of the performance of digital mammography systems. Med Phys 34(3):906–914

57. Monnin P, Gutierrez D, Bulling S et al (2005) A comparison of the imaging characteristics of the new Kodak Hyper Speed G film with the current T-MAT G/RA film and the CR 9000 system. Phys Med Biol 50(19):4541–4552
58. Morgan RH, Hodges PC (1945) An evaluation of automatic exposure control equipment in photofluorography. Radiology 45:588–593
59. Moses WW (2003) Time of flight in PET revisited. IEEE Trans Nucl Sci 50(5):1325–1330
60. Pan X, Sidky EY, Vannier M (2009) Why do commercial CT scanners still employ traditional, filtered back-projection for image reconstruction? Inverse Probl 25(12):123009
61. Pichler BJ, Wehrl HF, Kolb A et al (2008) Positron emission tomography/magnetic resonance imaging: the next generation of multimodality imaging? Semin Nucl Med 38(3):199–208
62. Radon J (1917) On the determination of functions from their integrals along certain manifolds. Ber Saechs Akad Wiss 69:262–277
63. Reader AJ, Zaidi H (2007) Advances in PET image reconstruction. PET Clin 2:173–190
64. Rhodes DJ, Hruska CB, Phillips SW et al (2011) Dedicated dual-head gamma imaging for breast cancer screening in women with mammographically dense breasts. Radiology 258(1):106–118
65. Rose A (1948) The sensitivity performance of the human eye on an absolute scale. J Opt Soc Am 38:196–208
66. Rossmann K, Wiley BE (1970) The central problem in the study of radiographic image quality. Radiology 96(1):113–118
67. Samei E, Badano A, Chakraborty D et al (2005) Assessment of display performance for medical imaging systems: executive summary of AAPM TG18 report. Med Phys 32(4):1205–1225
68. Samei E, Flynn MJ, Reimann DA (1998) A method for measuring the presampled MTF of digital radiographic systems using an edge test device. Med Phys 25(1):102–113
69. Schlyer D, Rooney W, Woody C et al (2004) Development of a simultaneous PET/MRI scanner. In: IEEE Nucl Sci Symp Conf Rec 3419–3421
70. Seguchi S, Aoyama T, Koyama S et al (2010) Patient radiation dose in prospectively gated axial CT coronary angiography and retrospectively gated helical technique with a 320-detector row CT scanner. Med Phys 37(11):5579–5585
71. Shaw R (1963) The equivalent quantum efficiency of the photographic process. J Photogr Sci 11:199–204
72. Smith-Bindman R, Lipson J, Marcus R et al (2009) Radiation dose associated with common computed tomography examinations and the associated lifetime attributable risk of cancer. Arch Intern Med 169(22):2078–2086
73. Townsend DW, Beyer T (2002) A combined PET/CT scanner: the path to true image fusion. Br J Radiol 75:S24–S30
74. Verdun FR, Theumann N, Poletti PA (2006) Impact of the introduction of 16-row MDCT on image quality and patient dose: phantom study and multi-centre survey. Eur Radiol 16(12):2866–2874
75. Wagner RF (1978) Decision theory and the signal-to-noise ratio of Otto Schade. Photogr Sci Eng 22:41–46
76. Wagner RF, Weaver KE (1972) An assortment of image quality indexes for radiographic film-screen combinations – can they be resolved? Appl Opt Instr Med Proc SPIE 35:83–94
77. Watson CC, Casey ME, Bendriem B et al (2005) Optimizing injected dose in clinical PET by accurately modeling the counting-rate response functions specific to individual patient scans. J Nucl Med 46(11):1825–1834
78. Webb S (1992) The physics of medical imaging. Institute of Physics, London
79. Weber MJ, Monchamp RR (1973) Luminescence of Bi4Ge3O12: spectral and decay properties. J Appl Phys 44:5495–5499
80. Xia T, Alessio AM, De Man B et al (2012) Ultra-low dose CT attenuation correction for PET/CT. Phys Med Biol 57(2):309–328
81. Xu J, Mahesh M, Tsui BM (2009) Is iterative reconstruction ready for MDCT? J Am Coll Radiol 6(4):274–276

82. Zaidi H (ed) (2006) Quantitative analysis in nuclear medicine imaging. Springer, New York
83. Zaidi H (2007) Is MRI-guided attenuation correction a viable option for dual-modality PET/MR imaging? Radiology 244(3):639–642
84. Zaidi H (2007) Is radionuclide transmission scanning obsolete for dual-modality PET/CT systems? Eur J Nucl Med Mol Imaging 34(6):815–818
85. Zaidi H, Del Guerra A (2011) An outlook on future design of hybrid PET/MRI systems. Med Phys 38(10):5667–5689
86. Zaidi H, Hasegawa B (2003) Determination of the attenuation map in emission tomography. J Nucl Med 44(2):291–315